ACS OMEGA

Open Access

http://pubs.acs.org/journal/acsodf

Article

Occurrence Mechanism of the Abnormal Gelation Phenomenon of High Temperature Cementing Slurry Induced by a Polycarboxylic Retarder

Xiujian Xia, Hang Zhang, Yongjin Yu, Junxing Li, Yun Cheng, Pu Xu, Miaomiao Hu,* and Jintang Guo*

Cite This: *ACS Omega* 2024, 9, 9424−9431

Read Online

ACCESS | Metrics & More | Article Recommendations

ABSTRACT: The class G oil well cement is a type of special cement that can be subjected to a high temperature formation environment. It was found that the class G cement tail slurry with a low polycarboxylic retarder dosage (usually ≤1% by weight of cement) was more prone to cause the abnormal gelation phenomenon (AGP) than the lead slurry with a high retarder dosage at a high temperature (usually when $T \geq 120$ °C). This study aimed at the occurrence mechanism of this unfavorable phenomenon that seriously endangers the cementing security. Results showed that the abnormal gelatinous region underwent premature hydration; namely, the calcium hydroxide and calcium silicate hydrate (C−S−H) content were all higher than the nongelatinous region, while the copolymer content was the opposite. Correspondingly, the theory of "premature hydration and crystal nucleation" was proposed to explain the abnormal gelation mechanism of a cementing tail slurry with an insufficient retarder dosage. Furthermore, a novel functionalized copolymer retarder "PAIANS" was synthesized to alleviate the AGP.

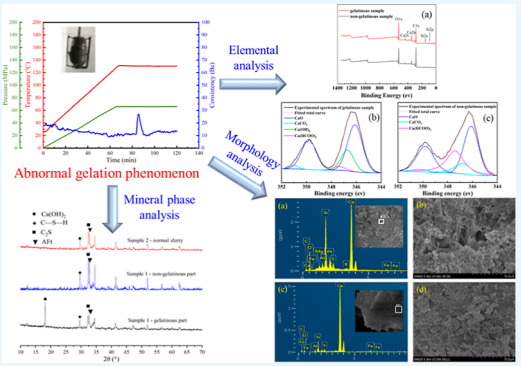

1. INTRODUCTION

With the gradual decrease of petroleum and gas recoverable reserves, the exploration and extraction of oilfields has developed toward deep or ultradeep wells, which has brought many challenges into cementing engineering.[1−3] In the oil and gas well cementing construction, the cement slurry is injected into the wellbore casing and returns up from the annulus area between the casing and the formation.[4,5] This process requires the slurry to maintain a normal flow state without abnormal phenomena such as "flash setting", "early setting", and "abnormal gelation". In recent years, with the gradual increase in the number of deep wells, the application temperature of cement slurry has also increased.[6] Therefore, it is necessary to introduce a number of organic copolymer additives into the oil well cement slurry systems to regulate their performances and ensure the quality and safety of cementing construction.[7−10]

Retarder is a necessary additive to guarantee the pumping safety of an oil well cement slurry. Currently, the commonly used oil well cement retarders mainly include lignosulfonates,[11,12] hydroxyl carboxylic acids,[13,14] organic phosphonates,[15] and 2-acrylamido-2-methylpropanesulfonic acid (AMPS)-based polycarboxylic copolymers.[16,17] Among which, the AMPS-based polycarboxylic copolymer retarder is most commonly used in the high temperature cementing due to its excellent thermal resistance and designable molecular structure, which has become a research hotspot for domestic and foreign petroleum workers.[13,17−19] At present, the commonly used polycarboxylic retarders are mainly composed of monomers such as AMPS, acrylamide (AM), itaconic acid (IA), maleic acid, organophosphonic acid, and their derivatives, which are synthesized by free radical copolymerization.[20−24] This type of retarder achieves the aim of inhibiting the oil well cement hydration at high temperatures through its strong adsorption and complexation behavior.[16,25]

However, it has been found both in laboratory research and field application that the addition of polycarboxylic additives could lead to abnormal thickening behaviors of oil well cementing slurry systems at high temperature, such as rapid thickening, abnormal gelation phenomenon (AGP), thickening time inversion, and so on.[26−28] In laboratorial research, the thickening experiment is commonly utilized to monitor the flow state changes of cement slurry during its dynamic hydration reaction and draws a thickening curve to record the real-time consistency value of the slurry (unit: Bc[29]). Under normal circumstances, the thickening curve of the cement slurry should be smooth. When the cement slurry is set, its consistency will rise to 100 Bc in a short time. Once the

Received: November 8, 2023
Revised: January 8, 2024
Accepted: February 2, 2024
Published: February 19, 2024

AGP occurred during the thickening process, it could be observed in the thickening curve as the consistency increased sharply and then dropped down[14] (see Figure 1), which was

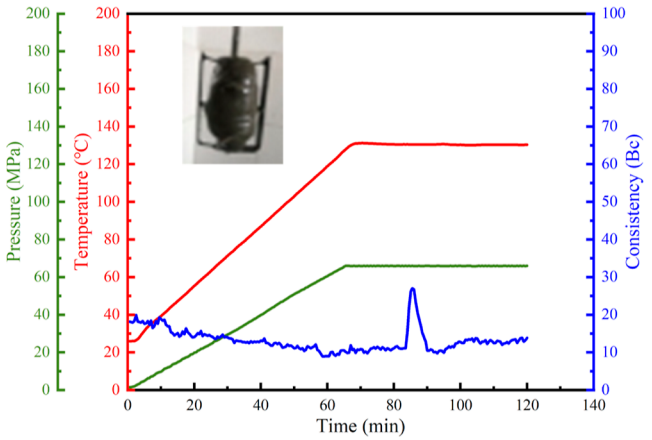

Figure 1. Thickening curve of abnormal gelatinous cement slurry.

due to the fact that the stirring paddle was wrapped by a layer of gelatinous cement slurry. This phenomenon would significantly deteriorate the cementing quality and bring risks to pumping operations in the construction field. Since the annulus size between the casing and the bore lining is small (3−5 cm),[30] accordingly the addition of retarder in the tail slurry is generally small. During the injection process of the slurry, the AGP of cementing tail slurry usually tends to occur due to the increase of temperature (usually when $T \geq 120$ °C) and too little polycarboxylic retarder (usually ≤1% bwoc). The gelatinous cement slurry adhered to the wellbore and casing string surface and accumulate continuously. The gelatinous cement aggregates are likely to block the annulus and affect the safety of cementing construction. In severe cases, it would cause "flagpole insertion" accident,[31] which is a figurative portrayal of the gelatinous cement trapped in the wellbore and could also be reflected in the thickening experiment (see Figure 1 inset picture). This phenomenon would incur pump choke and hinder further pumping of the cement slurry, thereby leading to cementing failure. Moreover, the accumulated abnormal gelatinous slurry could result in the heterogeneity of the slurry and the stratification phenomenon after setting, which seriously affects the structural integrity and sealing integrity of the cement paste.[32] Thereby, it is of great practical significance to investigate the occurrence mechanism of the abnormal gelation behavior of the oil well cement tail slurry under a low retarder dosage.

By means of XRF, XRD, XPS, SEM-EDS, TOC, and GPC, the theory of "premature hydration and crystal nucleation" was proposed to explain the abnormal gelation behavior of an oil well cement tail slurry with an insufficient dosage of retarder. Furthermore, a novel functionalized copolymer PAINS was synthesized to solve the AGP.

2. EXPERIMENTAL SECTION

2.1. Materials. AMPS was obtained from Ruibolong Petroleum Technology (Beijing, China). IA and acrylic acid (AA) were bought from the JiangTian chemical industry (Tianjin, China). Sodium *p*-styrenesulfonate (SSS) and ammonium persulfate (APS) were bought from Dibo Biotechnology Co., Ltd. (Shanghai, China). *N*-Vinyl-2-pyrrolidinone (NVP) was obtained from Jiaozuo Zhongwei special products pharmaceutical Co., Ltd. (Henan, China). The class G oil well cement was acquired from Jiahua Special Cement Co., Ltd. (Sichuan, China). Its mineral composition (using Rietveld refinement method based on XRD measurement) and basic physical properties (determined by laser particle size analyzer using dry dispersion method) are shown in Table 1.

2.2. Sample Preparations. *2.2.1. Preparation of Polycarboxylic Copolymer Retarders.* Two polycarboxylic retarders were synthesized in this work, whose names and feeding mass ratios were (I) PAIA (AMPS/IA/AA = 8:1:1) and (II) PAIANS (AMPS/IA/AA/NVP/SSS = 6.5:0.5:0.75:1:1.25). Their synthetic methods were the same; an example of the synthetic process of PAIANS was as follows. First, all acidic monomers (AMPS, IA, and AA) were dissolved into deionized water, and then, the pH value of the system was adjusted to 3 using 40 wt % NaOH solution. Subsequently, the remaining functional monomers NVP and SSS were added to the system. Finally, the mixed solution was poured into a three-necked flask and preheated to 60 °C in a water bath. Followed by the addition of initiator APS (0.5 wt %, by weight of monomers), the reaction system was kept polymerization at 60 °C for 3 h. The solid content of the final retarder PAINM solution was 30 wt %.

2.2.2. Preparation of Oilwell Cement Slurry. According to Section 5 of ref 33 (Preparation of Slurry) of the API Recommended Practice 10 B-2 "Recommended Practice for Testing Well Cements",[33] cement slurry with the density of 1.90 g/cm^3 was prepared using a Waring blender (OWC-2000D, Shenyang TaiGe). In order to investigate the correlation between retarder (single variable) and AGP, and to exclude the potential impact brought by other additives, the cement slurry composition in this work included only cement, retarder, and water. The polycarboxylic copolymer PAIA [P(AMPS/IA/AA)] was used as retarder.[34] The water/cement ratio was controlled at 0.44 to keep the density of the cement slurry at 1.90 g/cm^3, which was in line with other studies in the cementing industry.[10,35] The cement was poured into water within 15 s as the blender stirred at low speed (4000 rpm) and then mixed for 35 s at high speed (12,000 rpm).

2.2.3. Thickening Experiment and Acquisition of Cement Samples. Based on Section 9 of ref 33 (Well-simulation Thickening Time Tests) of the API Recommended Practice 10 B-2[33] and the oil and gas industry standard SY/T5504.1−2013 "evaluation method for well cement additives: Part 1, Retarder",[36] the high-temperature and high-pressure consistometer (model 8040D, Chandler, USA) was used to evaluate the thickening performance of the cement slurry under the

Table 1. Basic Parameters of Class G Oil Well Cement

mineral composition, % wt						physical properties	
C_3S	C_2S	C_3A	C_4AF	gypsum	hemihydrate	d_{50}, μm	density, g/cm^3
55.89	24.39	2.30	14.35	1.95	1.12	16.00	3.24

https://doi.org/10.1021/acsomega.3c08885
ACS Omega 2024, 9, 9424−9431

condition of 120 °C and 60 MPa. The thickening phenomena of cement slurry with different dosages of retarder PAIA are listed in Table 2. When the AGP happened, the gelatinous and the nongelatinous parts of sample 1 were, respectively, collected from the early paused thickening experiment and freeze-dried. As a control, the normal cement slurry of sample 2 after pausing the thickening experiment was also collected and freeze-dried.

Table 2. Thickening Phenomena of Cement Slurry with Different Dosages of Retarder[a]

mark	polycarboxylic retarder	dosage (bwoc)	conditions (°C)	thickening phenomenon
sample 1	PAIA	1%	120	gelatinous
sample 2	PAIA	2%	120	normal

[a]"bwoc" represents by weight of cement.

2.3. Characterizations. *2.3.1. Component of Cement Samples.* The powder of gelatinous and nongelatinous samples was measured by XPS (American Thermal Science ESCALAB 250xi with Al Kα radiation) to quantitatively investigate the elemental content and valence state on the samples' surface. Then the data were processed by XPSPEAK software to recognize the chemical environment of the Ca element and identify the binding forms of Ca^{2+} with $-COO^-$ or $-OH^-$. Next, the powder samples were characterized by XRD (D8-Focus, BRUKER-AXS GmbH, Germany) with the 2θ scanning range from 10° to 70° at a rate of 10°/min, and the Cu target Kα radiation (λ = 0.154 nm) was utilized to test. Furthermore, the elemental content of the cement samples was investigated by XRF (Shimadzu Corporation, Japan). The morphology and elemental analysis of these samples were measured by SEM-EDS (S-4800, HITACHI, Japan).

2.3.2. Properties of Polycarboxylic Retarder. The adsorption property of the retarder was characterized by a total organic carbon analyzer (TOC-VCPN, SHIMADZU Company, Japan). The adsorptive capacity of retarder on the surface of oil well cement grains was calculated by the difference of organic carbon content between the raw liquid and the filtrate collected before and after the fluid loss test of the cement paste (depletion method).[12,37] According to the Section 10 of ref 33 (Static Fluid-loss Tests) of the API Recommended Practice 10B-2,[33] the fluid loss process was performed in a static fluid loss apparatus (model TG-71, Taige, China) by applying a pressure of 1000 psi to the fluid loss cell with nitrogen. Moreover, the synthesized retarder was characterized by FTIR (500 to 4000 cm^{-1}), TGA (30 to 600 °C at the rate of 10 °C/min), and GPC (0.1 M $NaNO_3$ solution as eluant whose flow rate was 0.5 mL/min).

3. RESULTS AND DISCUSSION

3.1. Mineral Phase Determination of AG and Non-AG Cement Samples. *3.1.1. XRD Analysis.* XRD curves of AG and non-AG regions of the oil well cement slurry with 1% retarder and the normal cement slurry with 2% retarder are shown in Figure 2. As could be seen, the peaks at 18, 29 and 33°, respectively, represented calcium hydroxide (CH, JCPDS 44-1481), calcium silicate hydrate (C−S−H, JCPDS 29-0374), and ettringite (AFt, JCPDS 41-1454), which suggested the three samples contained hydrated products.[38] The most obvious difference was that the peak of 18° in the gelatinous sample with 1% retarder was very high, while the non-gelatinous sample 1 and the sample 2 with 2% retarder did not contain CH. This result suggested that the gelatinous part occurred premature hydration and a large amount of portlandite crystal accumulated.

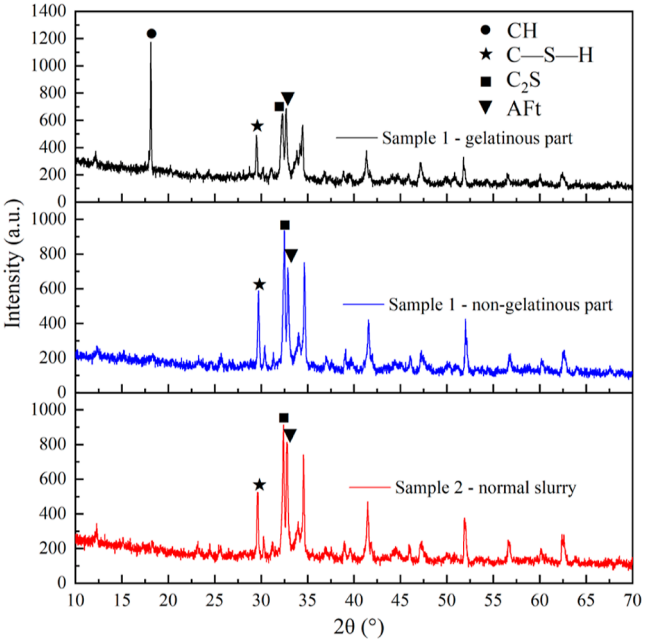

Figure 2. XRD curves of different oil well cement slurry sample powders.

3.1.2. XPS Analysis. XPS spectra of AG and non-AG samples are shown in Figure 3, and corresponding elemental compositions are listed in Table 3. As could be seen, the content of carbon in the nongelatinous sample (79.47%) was far more than that in the AG sample (59.30%), which indicated that the non-AG sample contains a large amount of polymer retarder and Ca^{2+} could be complexed by the polymers, so that the formation of CH crystal was inhibited. In contrast, the AG sample contained less retarder so that some extra Ca^{2+} aggregated and formed much CH crystal, which was consistent with XRD.

The chemical compositions of these two samples were very similar, except for the content of each element. The Ca 2p spectra were demonstrated in Figure 3b,c. We could see that the $CaCO_3$, $Ca(OH)_2$, CaO, and $Ca(HCOO)_2$ were the main compositions of the Ca 2p.[39] Apparently, the fitted curve of $Ca(HCOO)_2$ indicated the complexation of the retarder and Ca^{2+}. The content of $Ca(HCOO)_2$ could be expressed by the peak area ratio of $Ca(HCOO)_2$ and Ca 2p ($A_{Ca(HCOO)_2}/A_{Ca}$). Similarly, the content of $Ca(OH)_2$ was calculated by $A_{Ca(OH)_2}/A_{Ca}$. The higher the content of $Ca(HCOO)_2$, the stronger the complexation of retarder. From Figure 3b, we could obtain that the $A_{Ca(HCOO)_2}/A_{Ca}$ of the AG sample was 4.50%, and the $A_{Ca(OH)_2}/A_{Ca}$ of the AG sample was 19.60%. For comparison, Figure 3c showed that the $A_{Ca(HCOO)_2}/A_{Ca}$ of the non-AG sample was 24.98%, and $Ca(OH)_2$ was not found in the non-AG sample.

From the XPS data obtained above, it can be found that the content of $Ca(OH)_2$ in the AG sample was much higher than that in the non-AG sample, while the content of $Ca(HCOO)_2$ was much lower than that in the non-AG sample. Combined with the XRD results, it could be concluded that the AG

https://doi.org/10.1021/acsomega.3c08885
ACS Omega 2024, 9, 9424−9431

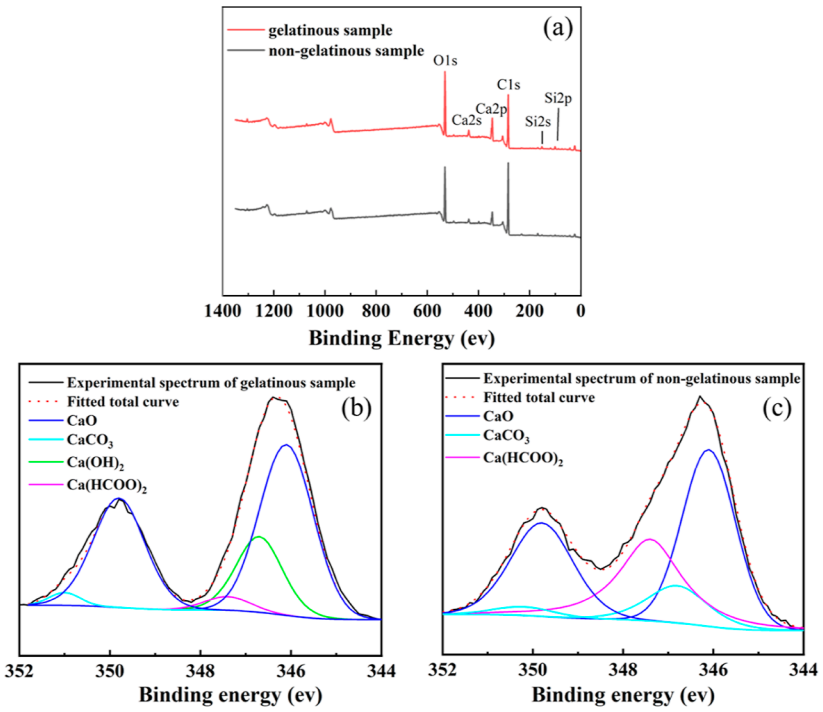

Figure 3. XPS (a) total spectra and Ca 2p fitted spectra of (b) gelatinous and (c) nongelatinous samples.

Table 3. Surface Elemental Composition (Atomic %) of AG and Non-AG Samples

element	C	O	Ca	Si
AG sample	59.30	31.44	3.28	5.98
non-AG sample	70.47	24.75	1.55	3.23

sample was formed by the aggregation of uncomplexed Ca^{2+} to form the CH crystal nucleus. With the growth of CH, the AG cement slurry was gradually formed under the shearing and stirring. In the non-AG sample, a large number of Ca^{2+} was complexed by polymer retarder so that the formation and growth of CH crystal nuclei was hindered.

3.1.3. XRF Analysis. The elemental compositions of AG and non-AG samples were characterized by XRF.[15] Table 4 showed that there was an obvious difference among the content of CaO and SiO_2 in the AG, non-AG sample, and oilwell cement. According to eq 1 below

$$\frac{(\mathrm{Si/Ca})_{\text{gelatinous}}}{(\mathrm{Si/Ca})_{\text{non-gelatinous}}} = \left(\frac{m\mathrm{SiO_2}}{m\mathrm{CaO}}\right)_{\text{gelatinous}} \times \left(\frac{m\mathrm{CaO}}{m\mathrm{SiO_2}}\right)_{\text{non-gelatinous}} \quad (1)$$

it could be calculated that the Si/Ca mass ratio of AG sample was 30.02%. Similarly, the non-AG sample was 13.54%, and the oil well cement was 17.20%. In conclusion, the Si/Ca ratio of the AG sample is more than twice as much as that of the non-AG sample. Obviously, a large amount of the hydrated silicate product accumulated in the AG sample.

3.1.4. SEM and EDS Analysis. The SEM and EDS characterizations of AG and non-AG samples are presented in Figure 4. Figure 4 exhibited a large amount of flaky CH on the surface of the AG sample since a large amount of Ca^{2+} was not complexed with a sufficient amount of retarder. In contrast, there was no CH on the surface of the non-AG samples (Figure 4d). The surface element content of the AG sample

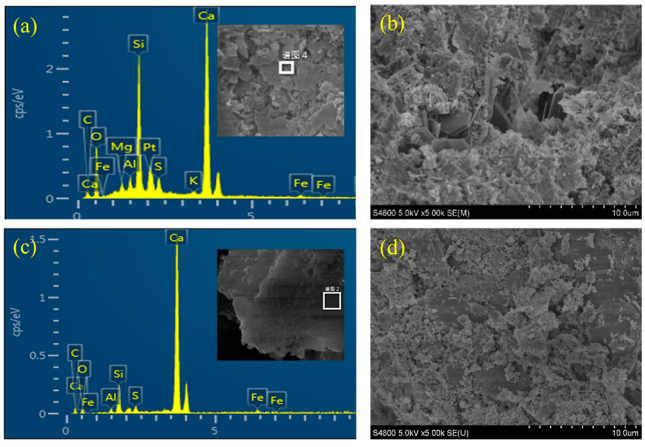

Figure 4. SEM images with EDS analysis of (a, b) AG and (c, d) nongelatinous samples.

Table 4. Elemental Analyses of Different Samples Determined by XRF (Mass Fraction,%)

species	CaO	SiO_2	Al_2O_3	Fe_2O_3	MgO	SO_3	K_2O	sum
AG sample	55.26	25.39	2.28	6.81	0.95	2.91	0.74	94.34
non-AG sample	68.36	14.90	2.50	6.70	0.99	2.90	0.61	96.96
class G oil well cement	66.14	17.41	2.30	6.78	0.99	2.90	0.74	97.26

https://doi.org/10.1021/acsomega.3c08885
ACS Omega 2024, 9, 9424−9431

Table 5. Element Content of AG and Non-AG Samples (Mass Fraction,%)

element	C	O	Al	Si	Ca	Fe	S	total
AG sample	5.28	29.41	1.35	14.13	46.02	1.79	2.02	100
non-AG sample	5.49	7.26	0.79	5.07	76.14	3.72	1.53	100

and non-AG sample is listed in Table 5. The Ca content of AG sample was much lower than non-AG sample, but the O content of AG sample was greater than the non-AG sample. This was because a large amount of Ca^{2+} in the AG sample prematurely hydrated to form CH so that the O content was increased.

3.2. Analysis of Polycarboxylic Retarder. *3.2.1. TOC Analysis.* In order to further illustrate the relationship between the retarder PAIA dosage and the AGP of cement slurry, the adsorptive behavior polycarboxylic retarder under different dosages was characterized by TOC.[40] Figure 5 shows that the

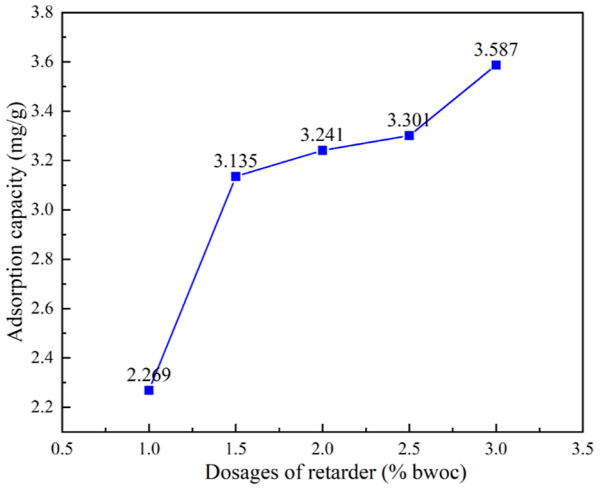

Figure 5. Relationship between adsorptive capacity of retarder and its dosages.

adsorptive amount of retarder gradually increased as its dosage increased. Since the cement grains could only provide finite adsorption sites, the anionic polymer would form a compact adsorption layer on the surface of cement while reaching the saturated adsorption point.[41,42] For the cementing tail slurry, the retarder of low dosage was far away from its equilibrium adsorption point; thereby, it could not form a dense and effective adsorption layer on the surface of cement grains to inhibit the premature hydration of cement minerals. In this case, the cement hydrated in advance and generated CH and C−S−H gel. Under the shearing and stirring, these hydration products wound on the stirring paddle and presented the AGP; for the lead slurry with a high retarder dosage, the increased polymer content could form a denser adsorption layer on the surface of cement grains than that with low retarder dosage; thus, it was able to hinder the premature hydration and less prone to abnormal gelation.

3.2.2. GPC Analysis. A series of experimental conditions were simulated to observe the relationship between the AGP and the molecular weight of retarder PAIA, and the results are listed in Table 6. Compared to the retarder at room temperature (M_n = 100,770), the number average molecular weight reduced approximately two-thirds (M_n = 32,170 in distilled water and M_n = 31,275 in alkaline environment) after being placed at 120 °C for 30 min.

Table 6. Molecular Weight Changes of Retarder PAIA Undergone Different Experimental Conditions: (No. 1) Room Temperature, (No. 2) Exposure to 120 °C for 30 min in Distilled Water, and (No.3) Exposure to 120 °C and pH 12 for 30 min

no.	Mn	Mw	M_w/M_n
1	100,770	456,197	4.527
2	32,170	174,185	5.414
3	31,275	90,119	2.882

The result indicated that some molecular chains of polycarboxylic retarder broke under high temperature exposure,[43] which led to the weakening of the complexation and adsorption effect. Therefore, for the tail slurry with low retarder dosage, its inhibitory effect on the premature hydration of cement was weakened, and the CH crystal and C−S−H gel were generated. For the lead slurry, although part of the molecular chains failed, the remaining molecular chains were still able to hinder the process of hydration through complexation and adsorption behaviors because of the high retarder dosage.

3.3. Occurrence Mechanism of AGP. According to the test results, we could see that there existed hydration differences between the AG and non-AG region. The AG region underwent premature hydration, which manifested as its CH crystal and C−S−H gel content were all higher than those of the non-AG region, while the copolymer content was the opposite. Hence, a theory of "premature hydration and crystal nucleation" was proposed to explain the effect of retarder dosages on the AGP. Specifically speaking, this theory was explained from two following aspects

(1) The complexation and adsorption effects of retarder in the tail slurry were weaker than the lead slurry. The low retarder content in the tail slurry was not able to sufficiently chelate Ca^{2+} and form an effective adsorption layer on the surface of the cement grains; thus, the cement minerals underwent premature hydration and generated CH crystal and C−S−H gel in advance, forming gelatinous cement slurry around the stirring paddle under the action of stirring and shearing. For the lead slurry with a high retarder dosage, the increased polymer content could fully inhibit the premature hydration of cement and thereby alleviating the AGP.

(2) The impact of temperature on the molecular properties of retarder. When the temperature reached 120 °C, a certain proportion of molecular chains of polycarboxylic retarder broke due to the reduced molecular weight under high temperature exposure, which weakened the complexation and adsorption behavior of the retarder. Therefore, for the tail slurry with low retarder dosage, the inhibitory effect on the premature hydration of cement weakened and the CH crystal and C−S−H gel were generated. For the lead slurry, although it also had a certain proportion of molecular chains broken, under the premise of high dosage, the remained molecular chains were enough to hinder the process of hydration

https://doi.org/10.1021/acsomega.3c08885
ACS Omega 2024, 9, 9424−9431

through complexation and adsorption behaviors. Therefore, the AGP would not occur.

3.4. Solution Method. According to Section 3.3, the high temperature environment broke the molecular chains of the polycarboxylic retarder and decreased its molecular weight. Therefore, two functional monomers (SSS and NVP) were introduced to alleviate the problem. These two monomers with rigid ring structure could eliminate the influence of molecular chain breakage.[16,27] On this basis, a five-membered copolymer PAIANS [P(AMPS/IA/AA/NVP/SSS)] was synthesized.

3.4.1. FT-IR Analysis of PAIANS. The FTIR spectrum of PAIANS is shown in Figure 6. As could be seen, the peaks at

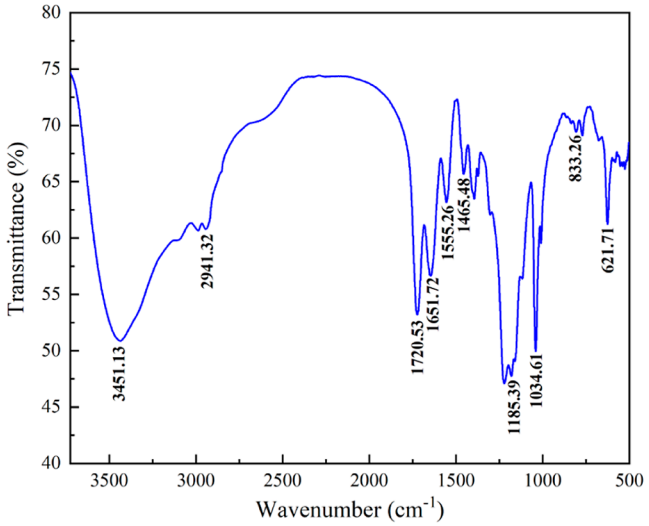

Figure 6. FTIR spectrum of the retarder PAIANS.

3451.13 and 621.71 cm^{-1} were the stretching vibration peaks of N−H in AMPS; 2941.32 cm^{-1} was the stretching vibration peak of-CH_2; 1651.72 cm^{-1} was the overlapping peak of −C═O in the AMPS amide bond and the −C═O in the NVP; 1185.39 and 1034.61 cm^{-1} were the symmetric and asymmetric stretching vibration absorption peaks of S═O[24] in the sulfonic acid group of AMPS; 1555 and 1486 cm^{-1} were the symmetric and antisymmetric stretching vibration peaks of $-COO^-$; 833.26 cm^{-1} was the characteristic peak of p-disubstituted benzene in the molecular structure of SSS;[44] and 1720 cm^{-1} was the absorption peak of C═O bond stretching vibration in IA. Moreover, the peak of C═C was absent among 1620 to 1640 cm^{-1}.[45] In summary, the FTIR analysis results contained each raw material monomer of the target product.

3.4.2. TGA-DTG Analysis of PAIANS. The TGA-DTG curves of PAIANS are shown in Figure 7. It was shown that the maximum thermal decomposition peak of PAIANS appeared at 350 °C, and the mass loss was only 5.6% before 350 °C which might be related to a small amount of oligomer in the product. The mass loss rate of PAIANS became faster beyond 350 °C and lost 44.6% before 400 °C. This huge mass loss indicated the small molecules that the polymer decomposed into underwent gasification. When the temperature reached above 400 °C, the mass loss rate slowed down and the polymer underwent further carbonization. To sum up, the TGA-DTG analytical results suggested a good thermal resistance of retarder PAIANS.

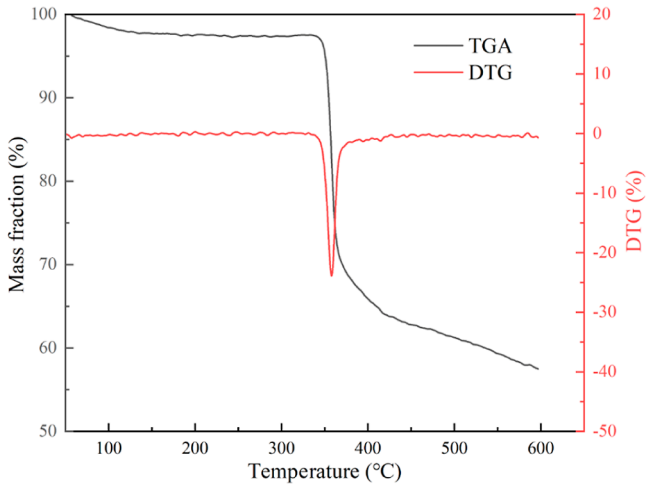

Figure 7. TGA-DTG curves of the retarder PAIANS.

3.4.3. GPC Analysis of PAIANS. For comparison with Section 3.2.2, the GPC determination of PAIANS under the same treatment conditions as PAIA was exhibited in Table 7. It

Table 7. Molecular Weight Changes of Retarder PAIANS Underwent Different Experimental Conditions: (No. 1) Room Temperature, (No. 2) Exposure to 120 °C for 30 min in Distilled Water, and (No. 3) Exposure to 120 °C and pH 12 for 30 min

no.	M_n	M_w	M_w/M_n
1	122,341	339,556	2.775
2	107,587	446,336	4.149
3	104,151	394,226	3.785

could be seen that the number-average molecular weight of experiments no. 2 and no. 3 decreased by 12.1 and 14.9%, respectively, compared to the control experiment no. 1 at room temperature. Combined with the GPC measurement results of PAIA in Table 6, we could see that the temperature resistance of PAIANS was significantly improved.

3.4.4. Thickening Performance Test of Cement Slurry with PAIANS. Both the laboratory study and field application have found that the AGP of cementing tail slurry at high temperature was prone to occur under a low retarder dosage (usually ≤1.5% bwoc).[46] Compared with the thickening performance of PAIA retarder in Table 2, the thickening performances of tail slurry with (a) 0.5% and (b) 1.0% bwoc retarder PAIANS at 120 °C/60 MPa are shown in Figure 8. As could be seen, the thickening curves were smooth without AGP occurring under 0.5 and 1.0% bwoc dosages of PAIANS. In conclusion, the AGP of cementing tail slurry could be relieved by properly increasing the carboxyl content and improving the thermal resistance of polycarboxylic retarder.

4. CONCLUSIONS

In this article, the occurrence mechanism of AGP of an oil well cement tail slurry with a low retarder dosage was studied. According to the test results, the AG cement slurry underwent premature hydration, specifically manifested as its CH and C−S−H content were all higher than the nongelatinous part, while the copolymer content was the opposite. Hence, a theory of "premature hydration and "crystal nucleation" was proposed. The explanations of this theory lay in two aspects: (1) the

https://doi.org/10.1021/acsomega.3c08885
ACS Omega 2024, 9, 9424−9431

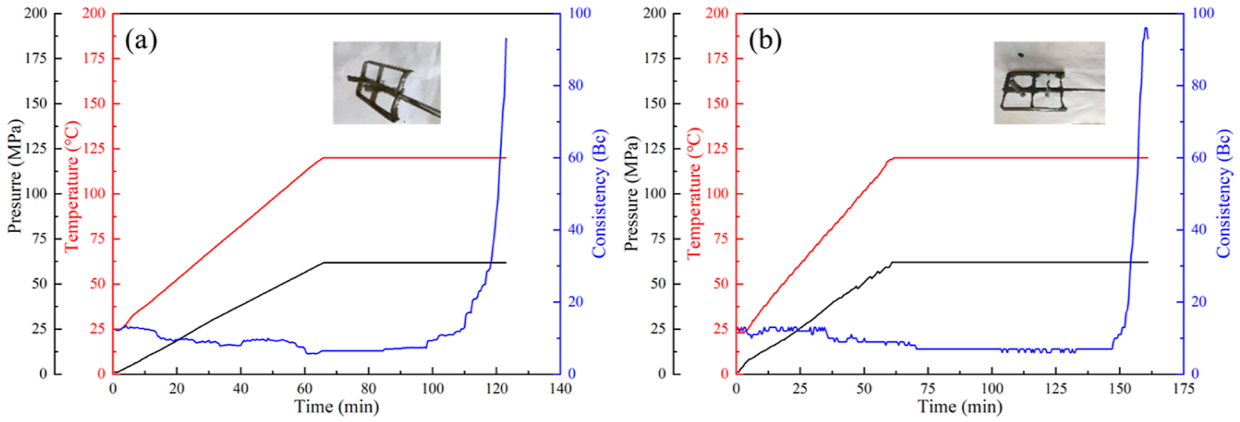

Figure 8. Thickening curves of oil well cement slurry with (a) 0.5% bwoc and (b) 1.0% bwoc retarder PAIANS.

complexation and adsorption effects of retarder in the tail slurry were weaker than those of the lead slurry. (2) The temperature increase to 120 °C reduced the molecular weight of retarder and weakened its complexation and adsorption ability.

In order to solve the problem of AGP, a novel functionalized copolymer PAIANS with a high temperature resistance and high carboxyl content was synthesized. It was found that the cement slurry with 0.5 and 1.0% bwoc PAIANS did not present AGP in the thickening tests. According to the test results, the conclusion could be obtained that the AGP of cementing tail slurry could be relieved by properly increasing the carboxyl content and improving the thermal resistance of polycarboxylic retarder.

AUTHOR INFORMATION

Corresponding Authors

Miaomiao Hu − *School of Chemical Engineering and Technology, Tianjin University, Tianjin 300350, China; Zhejiang Institute of Tianjin University (Shaoxing), Zhejiang 312300, China; Haihe Laboratory of Sustainable Chemical Transformations, Tianjin 300192, China;* orcid.org/0000-0002-1241-7167; Email: mmhu1990@tju.edu.cn

Jintang Guo − *School of Chemical Engineering and Technology, Tianjin University, Tianjin 300350, China; Zhejiang Institute of Tianjin University (Shaoxing), Zhejiang 312300, China; Haihe Laboratory of Sustainable Chemical Transformations, Tianjin 300192, China*; Email: jtguo@tju.edu.cn

Authors

Xiujian Xia − *CNPC Engineering Technology R&D Company Limited, Beijing 102206, China*

Hang Zhang − *School of Chemical Engineering and Technology, Tianjin University, Tianjin 300350, China*

Yongjin Yu − *CNPC Engineering Technology R&D Company Limited, Beijing 102206, China*

Junxing Li − *School of Chemical Engineering and Technology, Tianjin University, Tianjin 300350, China*

Yun Cheng − *School of Chemical Engineering and Technology, Tianjin University, Tianjin 300350, China*

Pu Xu − *CNPC Engineering Technology R&D Company Limited, Beijing 102206, China*

Complete contact information is available at: https://pubs.acs.org/10.1021/acsomega.3c08885

Notes

The authors declare no competing financial interest.

ACKNOWLEDGMENTS

This study was supported by the National Natural Science Foundation of China's Basic Science Center project (grant no. 52288101) and the Key Project of China National Petroleum Corporation (grant no. 2023DQ0529).

REFERENCES

(1) Lopez, E.; Olson, D.; Hunter, W. Method of cementing within a gas or oil well. U.S. Patent 7,967,909 B2, 2011.

(2) Roberto, B.; Flowers, J.; Cristopher, S. Compositions and methods for well cementing. EP 3344593 A1, 2018.

(3) Zhang, H.; Hu, M.; Li, P.; Liu, M.; Yu, Y.; Xia, X.; Liu, H.; Guo, J. Covalently bonded AMPS-based copolymer C S H hybrid as a fluid loss additive for oilwell saline cement slurry in UHT environment. *Constr. Build. Mater.* **2023**, *378*, 131177.

(4) Fatehi Marji, M.; Yousofian, H.; Soltanian, H.; Pourmazaheri, Y.; Abdollahipour, A. Superior crack propagation inhibitory effectiveness of MWCNT reinforced SBS toward improving oil/gas well cement integrity. *Constr. Build. Mater.* **2023**, *403*, 133171.

(5) Guo, S.; Bu, Y.; Lu, Y. Addition of tartaric acid to prevent delayed setting of oil-well cement containing retarder at high temperatures. *J. Pet. Sci. Eng.* **2019**, *172*, 269−279.

(6) Guan, X.; Wang, F.; Ren, Q.; Zheng, Y.; Mei, K. y.; Zhang, C.; Cheng, X. Preparation and mechanism of tartaric acid-intercalated hydrotalcite retarder for oil-well cement. *Constr. Build. Mater.* **2023**, *399*, 132580.

(7) Aïtcin, P.-C. Retarders. *Sci. Technol. Concr. Admixtures* **2016**, 395−404.

(8) Li, M.; Xie, D.; Guo, Z.; Lu, Y.; Guo, X. A Novel Terpolymer as Fluid Loss Additive for Oil Well Cement. *Int. J. Polym. Sci.* **2017**, *2017*, 1−8.

(9) Nadiv, R.; Vasilyev, G.; Shtein, M.; Peled, A.; Zussman, E.; Regev, O. The multiple roles of a dispersant in nanocomposite systems. *Compos. Sci. Technol.* **2016**, *133*, 192−199.

(10) Xu, Y.; Guo, J.; Chen, D.; Hu, M.; Li, P.; Yu, Y.; Zhang, H. Effects of amphoteric polycarboxylate dispersant (APC) and acetone formaldehyde sulfite polycondensate (AFS) on the rheological behavior and model of oil well cement pastes. *Colloids Surf., A* **2019**, *569*, 35−42.

(11) Pyatina, T.; Sugama, T.; Gill, S. Retarders' effects on some properties of class G cement cured at 80°C. *Adv. Cem. Res.* **2014**, *26* (4), 205−212.

(12) Recalde Lummer, N.; Plank, J. Combination of lignosulfonate and AMPS®-co-NNDMA water retention agent—An example for dual synergistic interaction between admixtures in cement. *Cem. Concr. Res.* **2012**, *42* (5), 728−735.

https://doi.org/10.1021/acsomega.3c08885
ACS Omega 2024, 9, 9424−9431

(13) Yu, Y.; Zhang, C.; Gu, T.; Xu, W.; Zhang, J.; Zhang, G.; Huang, S.; Liu, K.; Cheng, X. Synthesis and evaluation of a new type of oil-well cement temperature-resistant retarder. *Constr. Build. Mater.* **2021**, *302*, 124153.
(14) Sun, F.; Pang, X.; Kawashima, S.; Cheng, G.; Guo, S.; Bu, Y. Effect of tartaric acid on the hydration of oil well cement at elevated temperatures between 60 °C and 89 °C. *Cem. Concr. Res.* **2022**, *161*, 106952.
(15) Pang, X.; Boontheung, P.; Boul, P. J. Dynamic retarder exchange as a trigger for Portland cement hydration. *Cem. Concr. Res.* **2014**, *63*, 20−28.
(16) Zhang, H.; Hu, M.; Xu, Y.; Xia, X.; Zhang, C.; Yu, Y.; Feng, Y.; Guo, J. Inhibitory effects of functionalized polycarboxylate retarder on aberrant thickening phenomena of oil well cement at high temperature. *Constr. Build. Mater.* **2021**, *274* (121994), 121994.
(17) Guo, S.; Liu, H.; Shan, Y.; Bu, Y. The application of a combination of treated AMPS/IA copolymer and borax as the retarder of calcium aluminate phosphate cement. *Constr. Build. Mater.* **2017**, *142*, 51−58.
(18) Ma, C.; Bu, Y.; Chen, B. Preparation and performance of a lignosulfonate-AMPS-itaconic acid graft copolymer as retarder for modified phosphoaluminate cement. *Constr. Build. Mater.* **2014**, *60*, 25−32.
(19) Bu, Y.; Liu, H.; Nazari, A.; He, Y.; Song, W. Amphoteric ion polymer as fluid loss additive for phosphoaluminate cement in the presence of sodium hexametaphosphate. *J. Nat. Gas Sci. Eng.* **2016**, *31*, 474−480.
(20) Zhigang, P.; Jian, Z.; Qian, F.; Changjun, Z.; Yong, Z.; Bojian, Z.; Jinhua, H. Synthesis and retarder mechanism study of a novel amphoteric composite high temperature-resistant retarder for oil well cement. *RSC Adv.* **2018**, *8* (27), 14812−14822.
(21) Lu, Y.; Li, M.; Guo, Z.; Guo, X. A novel high temperature retarder applied to a long cementing interval. *RSC Adv.* **2016**, *6* (17), 14421−14426.
(22) Liu, H.; Bu, Y.; Ma, R.; Guo, W. Improve the practicability of calcium aluminate phosphate cement as well cement: The application of amphoteric ion polymer as retarder. *Constr. Build. Mater.* **2019**, *199*, 207−213.
(23) Xia, X.; Guo, J.; Chen, D.; Feng, Y.; Yu, Y.; Jin, J.; Liu, S. Hydrophobic associated copolymer as a wide temperature range synthetic cement retarder and its effect on cement hydration. *J. Appl. Polym. Sci.* **2017**, *134* (35), No. e45242.
(24) Tang, X.; Yang, Y.; Hu, X. Retarder design for long open-hole well cementing through the interfacial adsorption. *Colloids Surf., A* **2023**, *677*, 132278.
(25) von Daake, H.; Stephan, D. Adsorption kinetics of retarding admixtures on cement with time controlled addition. *Cem. Concr. Res.* **2017**, *102*, 119−126.
(26) Guo, S.; Bu, Y.; Liu, H.; Guo, X. The abnormal phenomenon of class G oil well cement endangering the cementing security in the presence of retarder. *Constr. Build. Mater.* **2014**, *54*, 118−122.
(27) Chen, D.; Guo, J.; Xia, X.; Yu, Y.; Jin, J.; Xu, M.; Liu, S.; Feng, Y. Abnormal gelation phenomenon of Class G oil well cement incorporating polycarboxylic additives and its countermeasures. *Constr. Build. Mater.* **2017**, *149*, 279−288.
(28) Gu, G.; Yao, X.; Zhou, X.; Xiao, L.; Wang, P.; Wang, D. Analysis of abnormal thickening behavior of the class G high sulfate resistance oil well cement. *Drill. Fluid Completion Fluid* **2015**, *32* (5), 49−53.
(29) Sun, L.-J.; Pang, X.-Y.; Ghabezloo, S.; Yan, H.-B. Modeling the hydration, viscosity and ultrasonic property evolution of class G cement up to 90 °C and 200 MPa by a scale factor method. *Pet. Sci.* **2023**, *20*, 2372−2385.
(30) Duan, X.; Li, S.; Jiang, X.; Chen, X. Analysis of oil-well cement paste aberrant gelation caused by polycarboxylic acid. *J. Daqing Pet. Inst.* **2011**, *35* (5), 79−83.
(31) Dang, D.; Xu, W.; Yang, J.; He, J.; Fei, Z.; Jiang, S.; Lu, S. Pressure-controlled cement plug injection technology with ultra-high-density cement slurry in well Hetan 1. *Oil Drill. Prod. Technol.* **2023**, *45* (3), 284−288.
(32) Wang, J.; Zhang, W.; Song, L.; Wu, J.; Wu, Y. Study on sealing integrity of cement sheath in ultra deep well reservoir reconstruction. *Energy Sci. Eng.* **2023**, *11* (7), 2630−2641.
(33) American Petroleum Institute. *"Recommended Practice for Testing Well Cements"*, API Recommended Practice 10B-2; American Petroleum Institute: WA, 2013.
(34) Guo, J.; Xia, X.; Liu, S.; Jin, J.; Yu, Y.; Yu, Q. A high temperature retarder HTR-300L applied in long cementing interval. *Pet. Explor. Dev.* **2013**, *40* (5), 656−660.
(35) Feng, Q.; Li, X.; Peng, Z.; Zheng, Y. Synthesis and performance evaluation of polycarboxylate dispersant for oil well cement. *Colloids Surf., A* **2023**, *662*, 131007.
(36) National Energy Administration, P. R. C. *Evaluation method for well cement additives - Part 1: Retarder*, SY/T 5504.1−2013; Petroleum Industry Press: Beijing, 2013.
(37) Cao, L.; Guo, J.; Tian, J.; Xu, Y.; Hu, M.; Guo, C.; Wang, M.; Fan, J. Synthesis, characterization and working mechanism of a novel sustained-release-type fluid loss additive for seawater cement slurry. *J. Colloid Interface Sci.* **2018**, *524*, 434−444.
(38) Zhang, H.; Zhuang, J.; Huang, S.; Cheng, X.; Hu, Q.; Guo, Q.; Guo, J. Synthesis and performance of itaconic acid/acrylamide/sodium styrene sulfonate as a self-adapting retarder for oil well cement. *RSC Adv.* **2015**, *5* (68), 55428−55437.
(39) Wang, M.; Wang, R.; Zheng, S.; Farhan, S.; Yao, H.; Jiang, H. Research on the chemical mechanism in the polyacrylate latex modified cement system. *Cem. Concr. Res.* **2015**, *76*, 62−69.
(40) Plank, J.; Lummer, N. R.; Dugonjić-Bilić, F. Competitive adsorption between an AMPS®-based fluid loss polymer and Welan gum biopolymer in oil well cement. *J. Appl. Polym. Sci.* **2010**, *116*, 2913.
(41) Chen, D.; Guo, J.; Xu, Y.; Hu, M.; Li, P.; Jin, J.; Yu, Y. Adsorption behavior and mechanism of a copolymer used as fluid loss additive in oil well cement. *Constr. Build. Mater.* **2019**, *198*, 650−661.
(42) Tiemeyer, C.; Lange, A.; Plank, J. Determination of the adsorbed layer thickness of functional anionic polymers utilizing chemically modified polystyrene nanoparticles. *Colloids Surf., A* **2014**, *456*, 139−145.
(43) Abousnina, R.; Manalo, A.; Lokuge, W.; Zhang, Z. Effects of light crude oil contamination on the physical and mechanical properties of geopolymer cement mortar. *Cem. Concr. Compos.* **2018**, *90*, 136−149.
(44) Mizuse, K.; Hasegawa, H.; Mikami, N.; Fujii, a. A. Infrared and Electronic Spectroscopy of Benzene-Ammonia Cluster Radical Cations [C6H6(NH3)1,2]+: Observation of Isolated and Micro-solvated σ-Complexes. *J. Phys. Chem. A* **2010**, *114*, 11060−11069.
(45) Xue, Z.; Hu, M.; Miao, X.; Zang, L.; Guo, J. Synthesis of a hydrophobic associating polymer and its application in plugging spacer fluid. *RSC Adv.* **2022**, *12* (18), 11402−11412.
(46) Lv, B.; Zhang, J.; Xie, S.; Liu, Z.; Zhu, J.; Xu, M. Synthesis and Evaluation of Highly Inhibitory Oil Well Cement Retarders with Branched-Chain Structures. *ACS Omega* **2023**, *8* (43), 40754−40763.

https://doi.org/10.1021/acsomega.3c08885
ACS Omega 2024, 9, 9424−9431